

# FESTKORPERPROBLEME XX

---

## ADVANCES IN SOLID STATE PHYSICS

*Volker Dohm, Reinhard Folk*  
Critical Dynamics near the  $\lambda$ -Transition in  $^4\text{He}$

*Charles B. Duke*  
Organic Solids: Traditional Semiconductors or Fermi Glasses?

*Martial Ducloy*  
Nonlinear Optical Phase Conjugation

*Klaus Schulten*  
Magnetic Field Effects in Chemistry and Biology

*Jan Tauc*  
Photoinduced Absorption in Amorphous Silicon

*Matthias Scheffler*  
Electronic Structure of Simple Deep-Level Defects in Semiconductors

*Hartmut Haug*  
Nonlinear Optical Phenomena and Bistability in Semiconductors

*Lester F. Eastman*  
Very High Electron Velocity in Short Gallium Arsenide Structures

*Wolfgang Henning*  
Semiconductor Microelectronic Sensors

*Ralf Dornhaus*  
Surface Enhanced Raman Spectroscopy

*Heiner Köstlin*  
Application of Thin Semiconductor and Metal Films in Energy Technology

*Horst Hoffmann*  
Thin Metal Films: Two and Three Dimensional Behavior of Charge Carriers

*Frank Forstmann, Rolf R. Gerhardt*  
Metal Optics Near the Plasma Frequency

For reference to this article, please quote:

(Author, title), in: Festkörperprobleme (Advances in Solid State Physics), Volume XXII, page number, J. Treusch (ed.), Vieweg, Braunschweig 1982

## Magnetic Field Effects in Chemistry and Biology\*

Klaus Schulten

Physikdepartment, Technische Universität München, Garching, Federal Republic of Germany

**Summary:** Chemical and biological photoprocesses which involve bimolecular reactions between non-zero spin intermediates, e.g. doublet molecules  $^2\text{A} + ^2\text{B}$ , often produce the intermediate molecular pair in a pure overall spin state, e.g. a singlet state  $^1(^2\text{A} + ^2\text{B})$ , and select for the reaction channels again such spin states, e.g. a triplet state  $^3(^2\text{A} + ^2\text{B})$ . The necessary transition  $^1(^2\text{A} + ^2\text{B}) \rightarrow ^3(^2\text{A} + ^2\text{B})$  is affected by magnetic interactions (hyperfine, Zeeman, zero field splitting) and can be influenced by magnetic fields. Examples are photoinduced electron transfer processes, e.g. the primary reaction of photosynthesis.

### 1 Introduction – Magnetic Field Effects on Chemical Systems

The study of possible influences of magnetic fields on chemical and biological processes with claims of rather odd effects had been for long an activity of ill repute; the proponents of this activity were those unable to comprehend a simple argument: the strength of magnetic interactions is much smaller than thermal energies  $kT$  and, hence, on thermodynamic grounds chemical and biological processes cannot be influenced by magnetic fields to any measurable degree.

This argument appears to be completely valid. However, it has to be realized that a chemical reaction cannot only be affected by alterations of potential energy surfaces through external forces but also by the perturbation of a coherent quantum mechanical process, for which purpose interactions much weaker than  $kT$  will suffice. In fact, there had been a variety of observations [1] which demonstrated by means of altered intensities in NMR and ESR spectra that chemical reactions can lead to products with electron (in case of doublets) and nuclear spins strongly perturbed from their nearly uniform thermal orientational distribution. The correct explanation of this phenomenon [1] involves the occurrence of a pair of doublet molecules in a pure singlet or triplet quantum state, the magnetic hyperfine interaction between electron and nuclear spins coherently altering the spin motion, i.e. mixing singlet and triplet states and concomitantly polarizing the nuclear spins (see below). This explanation known as 'Chemically Induced Dynamic Spin Polarization' opened the avenue for an experimental technique to detect chemical reaction routes involving doublet intermediates.

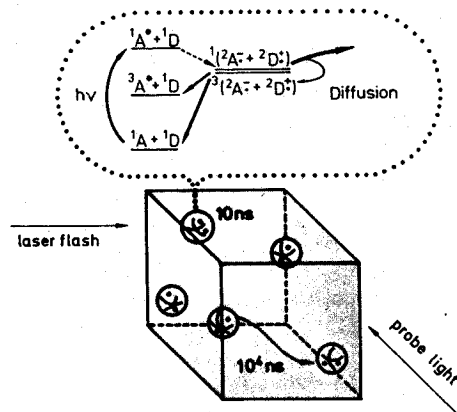
Our own interest [2] in the role of magnetic interactions in chemical processes came about through observations regarding the photochemical process illustrated in

\* Dedicated to A. Weller on the occasion of his 60th birthday.

Fig. 1: A polar liquid contains two kinds of molecules, electron acceptors A and electron donors D. The molecules selected, A = pyrene and D = dimethylaniline acquire the ability for electron transfer only after photoexcitation  $^1A \rightarrow ^1A^*$ . When  $^1A^*$  collides in the liquid with  $^1D$  an electron is transferred and the pair of doublets  $^2A^- + ^2D^+$  is formed. Energetically two routes are open for the back transfer, either to the ground state  $^1A + ^1D$  or to the triplet excited state  $^3A^* + ^1D$ . When we entered the field in 1975 a dispute raged if, in fact, a population of the  $^3A^*$  state had been observed as early as a few nanoseconds after photoexcitation and formation of the ionic doublets  $^2A^- + ^2D^+$ , and whether that would be physically possible at all. The point of the discussion was that the precursor of the doublet pair is a singlet state, i.e.  $^1A^* + ^1D$ , and, therefore, electron transfer creates the doublet pair also in a singlet alignment, i.e.  $^1(^2A^- + ^2D^+)$ . In case a third partner, either  $^2A^-$  or  $^2D^+$ , intercepts the original pair, the mutual electron spin alignment between the new reaction partners is random, i.e. 25 % singlet and 75 % triplet, and, hence, such events can populate the triplet state. However, because of the existing low concentration of doublets the mean time for such events to occur is about  $10^4$  ns. The claim of a triplet population  $^3A^*$  at considerably earlier times necessitates a magnetic perturbation which realigns the electron spins in the original  $^1(^2A^- + ^2D^+)$  pair. Because of the Brownian motion of the molecular partners the average time an ionic pair  $^2A^- + ^2D^+$  spends together in a close neighbourhood in a polar liquid is limited to a few nanoseconds and, hence, the magnetic interaction has to be effective in such short time. However, because the singlet and triplet alignments of a doublet pair not in direct contact, i.e. with negligible exchange interaction, are energetically degenerate a perturbation energy of  $10^{-7}$  eV suffices to produce a spin realignment on this time scale.  $10^{-7}$  eV is, in fact, the size of magnetic interactions, e.g. the hyperfine coupling in organic compounds or the Zeeman interaction for electron spins in fields of a few Gauss.

Fig. 1

Cyclic electron transfer in a polar liquid: the process is induced by a ns laser flash, the concentrations of the participating compounds  $^1A$ ,  $^3A^*$ ,  $^1A^*$ ,  $^1D$ ,  $^2A^-$  and  $^2D^+$  are monitored through their absorption spectra by means of a probe light; the initial electron transfer  $^1A_1^* + ^1D_1 \rightarrow ^2A_1^- + ^2D_1^+$  is followed by a reverse transfer either between the initial partners (i+i) or between random partners (i+r); the reverse transfer between the initial partners  $^2A_1^- + ^2D_1^+ \rightarrow ^1A_1 + ^1D_1$  has a duration of a few nanoseconds, after which time the initial pairs are irreversibly separated by Brownian motion; the subsequent reverse transfer between random partners  $^2A_1^- + ^2D_1^+ \rightarrow ^1A_1 + ^1D_1$  proceeds on a longer time scale of microseconds, the retardation being due to the low concentration of  $^2A^-$  and  $^2D^+$  which results in such long time for a random encounter to occur.



The dominant magnetic interaction in organic doublet molecules like pyrene and dimethylaniline is the hyperfine interaction between electron spins  $S_i$  and nuclear spins  $I_k^{(i)}$  separately in each molecule. The corresponding Hamiltonian is

$$H = H_1 + H_2$$

$$H_1 = \sum_k a_k^{(i)} S_i \cdot I_k^{(i)} = \bar{a} S_i \cdot \sum_k (a_k^{(i)}/\bar{a}) I_k^{(i)} \quad (1)$$

with isotropic hyperfine coupling constants  $a_k^{(i)}$ . For large nuclear spin systems with

comparable coupling constants  $a_k^{(i)} \approx \bar{a}$  one can treat  $I_i = \sum_k (a_k^{(i)}/\bar{a}) I_k^{(i)}$  approxi-

mately as a classical vector and view the hyperfine-induced spin motion as a precession of the electron spin  $S_i$  around the vector  $I_i$  with precession frequency  $(\bar{a}/2\hbar) I_i$  (see Fig. 2).

The semiclassical description of the hyperfine-induced electron spin motion just given [3] can readily incorporate the effect of an external magnetic field. The corresponding Zeeman interaction leads to the Hamiltonian ( $\mu$  is the Bohr magneton)

$$H_1 = \bar{a} S_i \cdot (I_i + (\mu g_i/\bar{a}) B), \quad (2)$$

i.e. the magnetic field vector adds to  $I_i$  (see again Fig. 2). This description neglects the Zeeman interaction on the nuclear spins which, however, is weaker by a factor  $< 10^{-3}$  and acts on a longer time scale not relevant for the ns electron spin dynamics. There exist further magnetic interactions which contribute to the relaxation of electron and nuclear spins, for example paramagnetic relaxation due to rotatio-

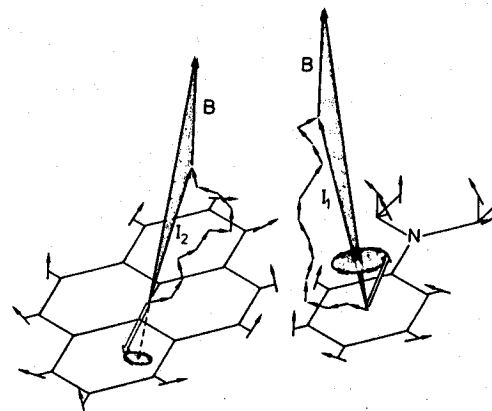


Fig. 2

Schematic illustration of the electron spin precession in the pyrene + N, N-dimethylaniline ( $^2A^- + ^2D^+$ ) doublet pair for a particular realization of nuclear spin orientations; the electron spin pair is shown in the initial singlet alignment  $^1(^2A^- + ^2D^+)$ ; only the spins of the  $^1H$  nuclei constituting the two molecules are presented, the nitrogen ( $^{14}N$ ) spin on the N, N-dimethylaniline is omitted, the carbon ( $^{12}C$ ) nuclei do not contribute to the hyperfine interaction since they carry nuclear spin zero, except in the case of the  $^{13}C$  isotope (from Ref. 3).

nal diffusion of the g-tensor and hyperfine coupling anisotropies. But again for organic radicals these interactions are weaker and contribute therefore only on timescales longer than the lifetime of the original ionic pairs.

Fig. 2 illustrates for a particular realization of nuclear spin orientations how the combined effect of Zeeman and hyperfine interaction produces a realignment of the electron spins in the pair  $^2A^- + ^2D^+$ , i.e. produces the transition  $^1(^2A^- + ^2D^+) \rightarrow ^3(^2A^- + ^2D^+)$ . Any observation will deal, however, with an ensemble of pairs  $^1(^2A^- + ^2D^+)$  with nearly uniform nuclear spin orientations. The resulting electron spin precession frequencies and axes vary in magnitude and orientation, respectively, and as a result one has to expect a strongly damped oscillatory transition  $^1(^2A^- + ^2D^+) \leftrightarrow ^3(^2A^- + ^2D^+)$ . Such behaviour is, in fact, born out by an exact quantum mechanical description of the electron spin motion of a pyrene – dimethylaniline doublet pair as shown in Fig. 3. This Figure does also provide a demonstration of the validity of the semiclassical description according to Fig. 2. The calculation predicts that in the absence of an external field doublet pairs starting with a singlet electron spin alignment will assume about 70 % triplet character after 5 ns, this percentage being reduced to 50 % and the time scale somewhat prolonged at fields of a few hundred Gauss. Hence, the calculations affirm the possibility of a fast (ns) population of the triplet state  $^3A^*$  along the route  $^1A^* + ^1D \rightarrow ^1(^2A^- + ^2D^+) \rightarrow ^3(^2A^- + ^2D^+) \rightarrow ^3A^* + ^1D$ . It was quite exciting when we also tested the second prediction that an external field should reduce the early population of  $^3A^*$ , but not the later phase of this population due to random encounter pairs  $^2A^- + ^2D^+$ .

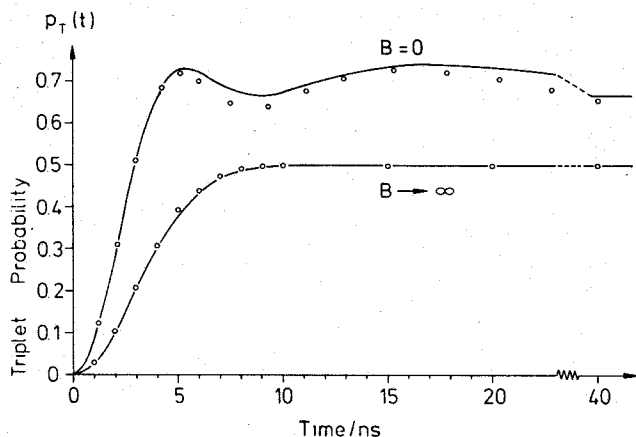


Fig. 3 Time development of the probability  $P_T(t)$  to find the initial  $^1(^2A^- + ^2D^+)$  doublet pair of Fig. 2 in a triplet state  $^3(^2A^- + ^2D^+)$ , i.e. either  $T_0, T_+, T_-$ ; (o) indicates the results of an exact quantum mechanical calculation, (—) indicates the semiclassical description of fixed nuclear spins as described in the text (from Ref. 3).

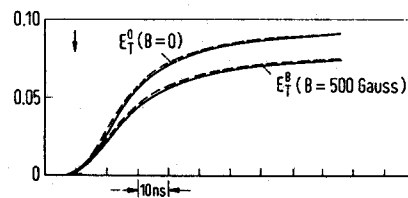


Fig. 4 Transient signals of the triplet ( $^3A^*$ ) absorption for the cyclic photoinduced electron transfer of pyrene + 3,5-dimethoxy-N,N-dimethylaniline in methanol (from Ref. 2); observations on the pyrene + dimethylaniline system can be found in Ref. 4.

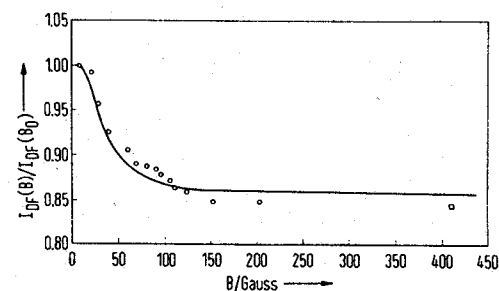


Fig. 5 Magnetic field dependence of the delayed fluorescence  $^3A^* + ^3A^* \rightarrow ^1A^* + ^1A$  of pyrene following photoinduced electron transfer of the system of Fig. 4, but obtained under stationary conditions; the delayed fluorescence intensities is a measure of  $[^3A^*]^2$ ; (o, □) represent the measurements; (—) represents the theoretical description (from Ref. 2).

Fig. 4 illustrates that the predicted field effect is being observed. In order to provide conclusive evidence regarding the origin of the early triplet population  $^3A^*$  we also examined the saturation behaviour of the magnetic field effect shown in Fig. 5. The explanation of this behaviour is the following: for  $(\mu g_i/\hbar) B \ll I_i$  the effect of the magnetic field according to the representation in Fig. 2 is negligible; around fields  $(\mu g_i/\hbar) B \approx I_i$  the variation of the effect is most pronounced; finally at fields  $(\mu g_i/\hbar) B \gg I_i$  the effect is saturated since in this regime the axis of spin precession is strictly along the direction of  $\underline{B}$  and it is only the constant component of  $\underline{I}_i$  along  $\underline{B}$  which contributes to the rephasing of the electron spins and, hence, to the transition  $^1(^2A^- + ^2D^+) \rightarrow ^3(^2A^- + ^2D^+)$ . The latter argument, however, applies only as long as the g-value difference  $g_1 - g_2$  in magnitude does not exceed values  $10^{-4} \dots 10^{-3}$ . For larger magnitudes one can expect another field dependence at fields of a few  $10^3$  Gauss. This dependence originates from the difference in the Zeeman interaction of the two electron spins  $\frac{1}{2} \mu (g_1 - g_2) B$  which results in different precession frequencies and, hence, in a realignment of the electron spins from  $S_0$  to  $T_0$ .

The spin motion described is altered in a most interesting way in case an electron spin is *not* residing permanently on a molecular moiety, but rather undergoes a paramagnetic – diamagnetic exchange, e.g. between two dimethylanilines  $^2D_1^+ + ^1D_2 \rightarrow ^1D_1 + ^2D_2^+$ . This situation is illustrated in Fig. 6. In this case the

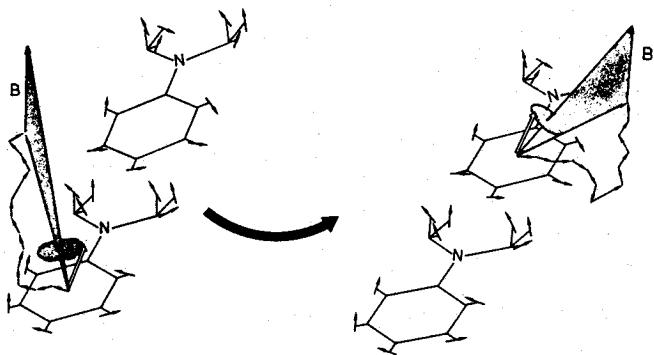


Fig. 6 Schematic illustration of the electron spin precession in the N, N-dimethylaniline ( ${}^2D^+$ ) doublet undergoing diamagnetic – paramagnetic exchange, i.e.  ${}^2D_1^+ + {}^1D_2 \rightarrow {}^1D_1 + {}^2D_2^+$  (from Ref. 3).

electron spin transferred finds a new random distribution of nuclear magnetic spins at its new residence  $D_2$  and, accordingly, will precess with altered frequency around a new axis. This opens the possibility to monitor and, in fact, quantitatively determine paramagnetic – diamagnetic exchange processes by means of the hyperfine coupling – induced singlet  $\rightarrow$  triplet transitions [3]. As a demonstration we present in Fig. 7 the time development of the triplet probability  $p_T(t, B)$  as altered due to the presence of paramagnetic – diamagnetic exchange. Relevant observations have been reported recently by two groups [5].

There is a complementary view of the spin motion as characterized by Figs. 2 and 6. This view is based on the energy level diagram for the electron spin pair in the presence of the Zeeman interaction alone. In this case the singlet state  $S_0$  and the triplet states  $T_0, T_+, T_-$  are eigenstates. The well-known magnetic field dependence of the energy levels is given in Fig. 8. The spin pair is initially prepared in the  $S_0$  state. The perturbation due to the hyperfine interaction at low field mixes the  $S_0$  and  $T_0, T_+, T_-$  states. One may expect that asymptotically the pair assumes an even distribution over all four states i.e. assumes  $\frac{1}{4}$  singlet and  $\frac{3}{4}$  triplet character. However, this is only approximately true. Inspection of the results in Fig. 3 and Fig. 7a reveals that the spin system asymptotically assumes only  $\frac{2}{3}$  triplet character. The reason is that the  $S_0$  and  $T_0, T_+, T_-$  states do not completely randomize due to the average over all nuclear spin orientations, there is, in fact, some ‘memory’ of the initial state. This is most clearly seen from Fig. 2 which shows that the electron spin component along the axis of precession is preserved in time whereas the perpendicular component oscillates in time. The averaging procedure annihilates the contribution of the latter to the overall spin state but does not do so for the parallel component. If, however, the axis of precession is subject to fluctuations arising from the

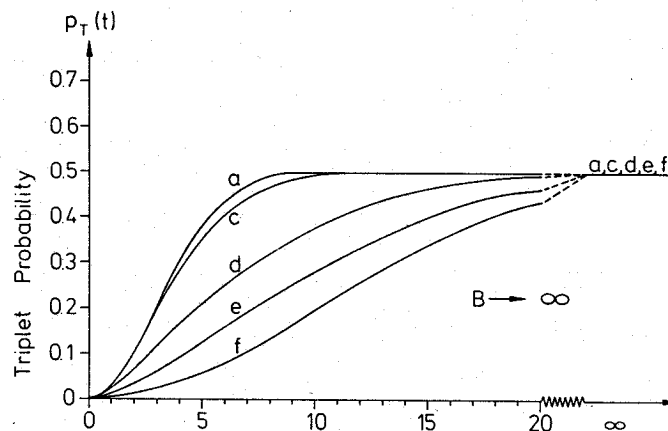
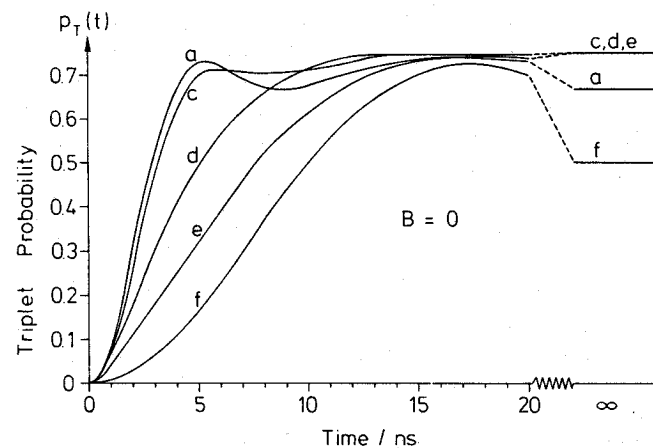


Fig. 7 Triplet probability of the doublet pair of Fig. 2 born in a singlet state ( ${}^1A^- + {}^2D^+$ ) in case of the paramagnetic – diamagnetic exchange of Fig. 6. The mean residence time of the unpaired electron spin on  ${}^2D^+$  was assumed to be (a)  $\infty$ , (c) 10 ns, (d) 1 ns, (e)  $1/3$  ns, (f) 0 ns (from Ref. 3).

paramagnetic-diamagnetic exchange (see Fig. 6) one expects a complete randomization and, an asymptotic triplet character of  $\frac{3}{4}$  as is indeed demonstrated in Fig. 7a.

The energy level diagram in Fig. 8 also leads to predictions about the expected magnetic field dependence of hyperfine coupling-induced singlet-triplet transitions, a subject matter discussed already briefly above. For this purpose one needs

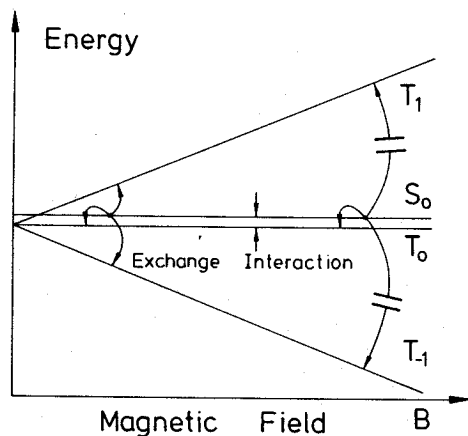


Fig. 8  
Splitting of the  $S_0$ ,  $T_0$ ,  $T_+$ ,  $T_-$  energy levels of a doublet pair  ${}^2A^- + {}^2D^+$  due to the Zeeman interaction; indicated is also the splitting between singlet and triplet levels due to an exchange interaction  $J(A-D)$ .

to compare the strength of the hyperfine interaction with the spacing between the  $S_0$  and the  $T_0$ ,  $T_+$ ,  $T_-$  levels. Very conveniently, the contribution  $a_k^{(i)}$  of each nuclear spin to the hyperfine interaction is generally given in units of Gauss, i.e. in terms of the magnetic field strength needed to separate the  $S_0$  and  $T_+$  ( $T_-$ ) levels by the energy value  $a_k^{(i)}$ . The root mean square value of the hyperfine interaction [3]

$$\left[ \sum_k a_k^{(i)2} I_k^{(i)} (I_k^{(i)} + 1) \right]^{1/2}$$

for pyrene and dimethylaniline amounts to about 10 Gauss and 32 Gauss, respectively, together to 42 Gauss. This leads one to expect that for fields  $B \gg 42$  Gauss the  $T_+$ ,  $T_-$  states are energetically so far removed from the  $S_0$  state initially prepared that according to the standard quantum mechanical argument these states cease to be coupled. As a result, the initial  $S_0$  state can only mix with the  $T_0$  state. In terms of the description of Fig. 2 this corresponds to the high field situation mentioned when the precession is strictly along the direction of  $\underline{B}$ . In this limit the spin motion does lead to an asymptotic equipartition between the available states  $S_0$  and  $T_0$ ,

i.e. the pair assumes at long times  $\frac{1}{2}$  triplet character, irrespective of paramagnetic-diamagnetic exchange processes (see Figs. 3, 7). This discussion explains then the observed field dependence of the triplet population as shown in Fig. 4: a reduction of the triplet population around fields of 42 Gauss and a saturation behaviour at higher fields. As a test of this supposition one can replace the hydrogen nuclei by deuterium, an isotopic substitution which is known to amount to a weakening of the hyperfine interaction. The deuterated compounds exhibit indeed a downfield shift of the field dependence [4].

On the basis of Fig. 8 one can also understand the important influence of the exchange interaction on the electron spin motion of a pair  ${}^2A^- + {}^2D^+$ . This interaction adds the term

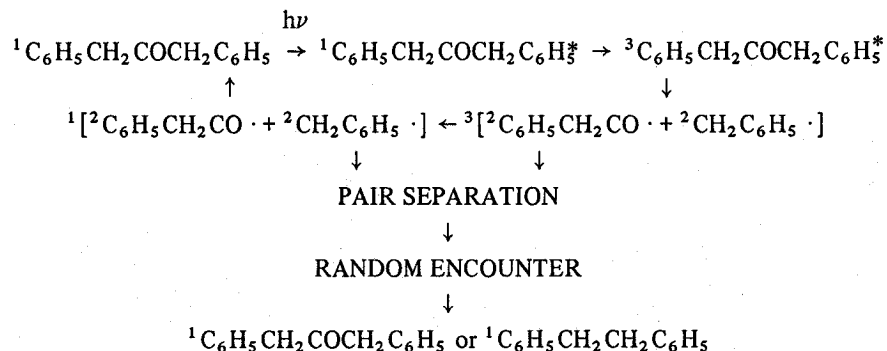
$$J(\underline{r}) \left[ \frac{1}{2} + 2\underline{S}_1 \cdot \underline{S}_2 \right] \quad (3)$$

to the spin Hamiltonian  $H = H_1 + H_2$ . The effect of the exchange interaction is to split the  $S_0$  and  $T_0$ ,  $T_+$ ,  $T_-$  levels by an amount  $2J(r)$  (see Fig. 8). The exchange energy  $J(\underline{r})$  depends on the overlap of the molecular orbitals carrying the electrons in the respective partners and, hence, depends sensitively on the distance  $r$  between  ${}^2A^-$  and  ${}^2D^+$ . One expects a variation of  $J(\underline{r})$  between values of the order 1 eV at close separations and zero when (several) liquid molecules are interspersed among  ${}^2A^-$  and  ${}^2D^+$ . The essential point is that the weak hyperfine interaction of  $10^{-6} - 10^{-7}$  eV can couple the  $S_0$  and the  $T_0$ ,  $T_+$ ,  $T_-$  states only in the case that  $J(\underline{r})$  does not exceed this weak interaction energy. In the case of the electron transfer events  ${}^1A^* + {}^1D \rightarrow {}^2A^- + {}^2D^+ \rightarrow {}^{1,3}A + {}^1D$  this implies that the partners  ${}^2A^-$  and  ${}^2D^+$  must clearly be separated for a few nanoseconds for the observed field effect to develop.

The magnetic field effect described is not just a curiosity but rather can be exploited to yield some hitherto unknown details of certain chemical and biological processes. We have already pointed out that the magnetic field effect selects only the population of  ${}^3A^*$  through the original pairs and does not include triplets through random encounters [6]. Hence, the magnetic field effect provides a window for pure pair processes in a liquid. Another aspect can be illustrated by means of Fig. 3 which shows that the spin realignment  ${}^1({}^2A^- + {}^2D^+) \rightarrow {}^3({}^2A^- + {}^2D^+)$  needs a certain time to develop. Hence, one expects that the magnetic field modulation of  ${}^3A^*$  depends sensitively on the lifetime of the original radical pair  ${}^2A^- + {}^2D^+$  in the liquid. For a lifetime of a few nanoseconds the triplet population at low and high fields is nearly proportional to the time integrals of the respective triplet probability curves in Fig. 3 and, therefore, the absolute magnetic field modulation provides a measure of the lifetime of the ionic pair.

The cyclic electron transfer process in Fig. 1 does not alter the chemical nature of the participating molecular partners. Because of its chemical inertness this system is most valuable for physical observations but most uninteresting for a chemist with a desire for chemical transformations. However, the appearance of doublet pairs in a pure electron spin state is rather common in chemistry. Hence, hyperfine-induced singlet  $\rightarrow$  triplet transitions beside being of great diagnostic value do also provide avenues for novel chemical techniques adding the magnetic field to the tool kit of chemistry. The fact that hyperfine coupling depends on the isotopic identity of the constituent atoms allows for new ways of isotope separation.

This point has been advanced by Turro and coworkers [7]. As an illustration we would like to discuss the reaction



This reaction involves an intermediate doublet pair born in the triplet state  ${}^3[{}^2\text{C}_6\text{H}_5\text{CH}_2\text{CO}\cdot + {}^2\text{CH}_2\text{C}_6\text{H}_5\cdot]$ . If rapid transition to the singlet state  ${}^1[{}^2\text{C}_6\text{H}_5\text{CH}_2\text{CO}\cdot + {}^2\text{CH}_2\text{C}_6\text{H}_5\cdot]$  is achieved the pair recombines to the starting material  ${}^1\text{C}_6\text{H}_5\text{CH}_2\text{COCH}_2\text{C}_6\text{H}_5$ . The triplet  $\rightarrow$  singlet transition can be much accelerated through the isotopic replacement  ${}^{12}\text{C} \rightarrow {}^{13}\text{C}$  of the carbon at the CO-group. If the triplet  $\rightarrow$  singlet transition is not achieved rapidly enough the pair  ${}^2\text{C}_6\text{H}_5\text{CH}_2\text{CO}\cdot + {}^2\text{CH}_2\text{C}_6\text{H}_5$  is likely to separate irreversibly, engage in random encounters and, thereby, reconstitute the starting material  ${}^1\text{C}_6\text{H}_5\text{CH}_2\text{COCH}_2\text{C}_6\text{H}_5$  as well as the new material  ${}^1\text{C}_6\text{H}_5\text{CH}_2\text{CH}_2\text{C}_6\text{H}_5$ . From this description the following observations can be readily explained: (1) there is a  ${}^{13}\text{C}$ -enrichment in the material  ${}^1\text{C}_6\text{H}_5\text{CH}_2\text{COCH}_2\text{C}_6\text{H}_5$ ; (2) the  ${}^{13}\text{C}$ -enrichment is reduced by an external field. Under appropriate conditions which involve the use of micellar reaction environments the photochemical process of Turro yields a  ${}^{13}\text{C}$ -enrichment of 1000 percent, i.e. provides an efficiency which is unrivalled by other known methods. The principle of magnetic isotope separation can be applied to other magnetic isotopes as well, including presumably  ${}^{235}\text{U}$ , if an appropriate chemical reaction is found.

## 2 Magnetic Field Effects on Photosynthetic Reactions

Photoinduced electron transfer reactions like in Fig. 1 happen to play a central role in biology in that they accomplish the primary process of photosynthesis. This process takes place in a membrane bound complex of proteins and pigments, the reaction center. In photosynthetic bacteria for which the system appears to be best known, e.g. in the bacterium *Rhodospseudomonas sphaeroides*, the reaction center functions like a photodiode at a p-n-junction. As shown schematically in Fig. 9 the valence (conduction) band of the biological photodiode is realized through the occupied (unoccupied) molecular orbitals of the following electron donor-acceptor groups arranged in a linear sequence: Cytochrome c; Bacteriochlorophyll

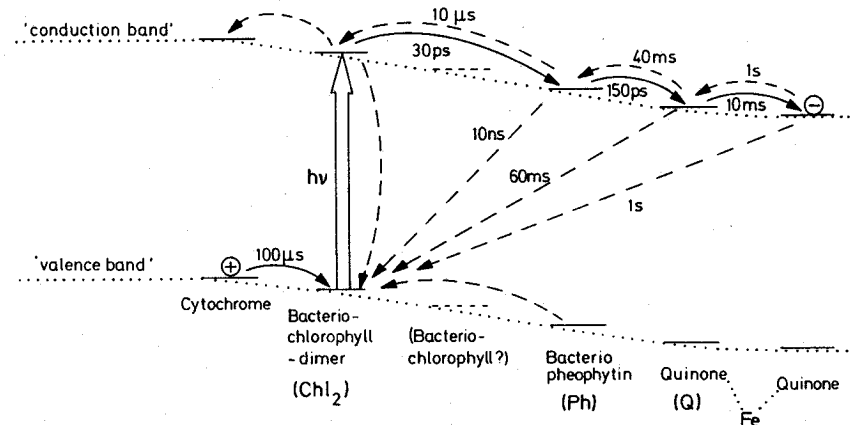
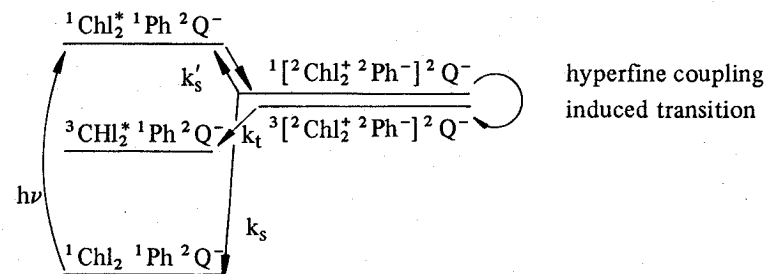


Fig. 9 Schematic presentation of the relevant molecular orbital energy levels of the constituent pigments of the bacterial photosynthetic reaction center to compare this system with a p-n-junction photodiode; the valence band is formed by the highest occupied orbitals, the conduction band by the lowest unoccupied orbitals; electronic excitation takes place at the bacteriochlorophyll - dimer in the center; (—) indicates the electron transfer processes favourable for the biological function, i.e. charge separation across the reaction center, (---) indicates processes unfavourable for this function (see text).

rophyll (presumably a dimer,  $\text{Chl}_2$ ); perhaps another Bacteriochlorophyll, omitted in the following discussion; Bacteriopheophytin (Ph); Quinone (Q); a second Quinone ( $Q'$ ). Q and  $Q'$  are associated with an Fe atom. The high efficiency of the reaction center photodiode is realized through an appropriate calibration of the electron transfer rates which are selected such that the favourable processes (—) compete well with the unfavourable processes (---). If the (presumable) second acceptor Q is reduced electrochemically, i.e.  ${}^1\text{Q} \rightarrow {}^2\text{Q}^-$ , the electron transfer chain in Fig. 9 is blocked and the photoinduced electron transfer will eventually be reversed. Just like in the 'in vitro' system in Fig. 1 two pathways are energetically possible for the reverse electron transfer, either to the singlet ground state or to a triplet excited state, depending on the momentaneous electron spin alignment of the  ${}^2\text{Chl}_2^+ + {}^2\text{Ph}^-$  pair:



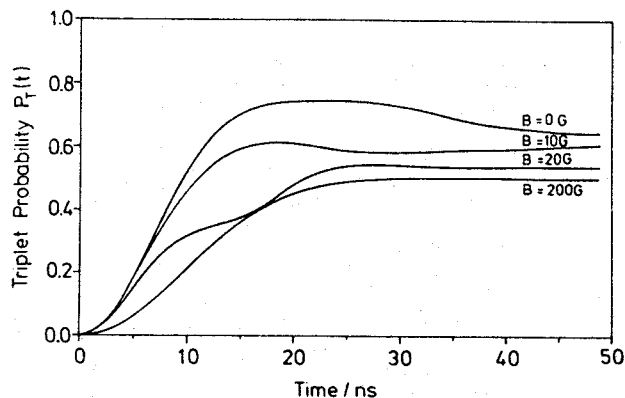


Fig. 10 Time evolution and magnetic field dependence of the triplet probability of a  ${}^2\text{Chl}_2^+ + {}^2\text{Ph}^-$  pair born in a singlet state (from Ref. 8).

In case the time scales of the electron transfer processes are in the nanosecond range one can expect a magnetic field behaviour very much like in the pyrene – dimethylaniline system. In fact, as shown in Fig. 10, a calculation like that of Fig. 3 applied to the  ${}^2\text{Chl}_2^+ + {}^2\text{Ph}^-$  pair reveals a similar time and magnetic field dependence of hyperfine coupling induced singlet  $\rightarrow$  triplet transitions. Since the root mean square values of the hyperfine interaction of  ${}^2\text{Chl}_2^+$  and  ${}^2\text{Ph}^-$  are 8 Gauss and 7 Gauss, respectively, i.e. less than for the pyrene – dimethylaniline pair, the singlet  $\rightarrow$  triplet transition takes somewhat longer to develop as compared to Fig. 3 and also exhibits a significant influence of fields as low as 10 Gauss. There is, however, an important difference to the chemical electron transfer system which derives from the 'solid state' character of the  ${}^2\text{Chl}_2^+ + {}^2\text{Ph}^-$  pair in the reaction center: the firm structure of the reaction center prevents a diffusive motion of the pair and also implies that all interactions which affect the electron spin precession, e.g. the exchange interactions between  ${}^2\text{Chl}_2^+$  and  ${}^2\text{Ph}^-$  as well as between  ${}^2\text{Ph}^-$  and  ${}^2\text{Q}^-$ , are presumably constant in time. Hence, one may expect contrary to the behaviour of the chemical system exemplified by Fig. 5 that the photosynthetic reaction center exhibits a magnetic field dependence of the  ${}^3\text{Chl}_2^*$  population which not only reveals the hyperfine interaction in  ${}^2\text{Chl}_2^+$  and  ${}^2\text{Ph}^-$  but other spin-dependent interactions as well. This is indeed borne out of observations by Hoff and collaborators illustrated in Fig. 11. The two measurements on two different preparations of the reaction center complex of *Rhodospseudomonas sphaeroides* reveal very different magnetic field behaviour. As the hyperfine coupling strength is the same for both systems the magnetic field behaviour should derive from differences in other interactions.

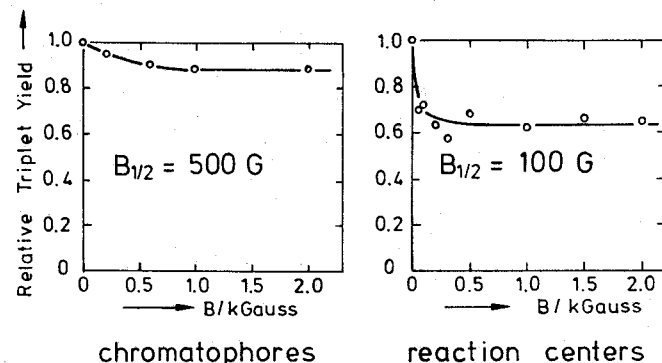


Fig. 11 Magnetic field dependence of the fraction of triplet population in the photosynthetic reaction center of *Rps. sphaeroides* as observed through triplet – triplet absorption of constituent carotenoid pigments (car); the carotenoid triplet states are populated through energy transfer  ${}^3\text{Chl}_2^* + {}^1\text{car} \rightarrow {}^1\text{Chl}_2 + {}^3\text{car}^*$ ; (a) whole chromophores, (b) isolated reaction centers (from Ref. 9).

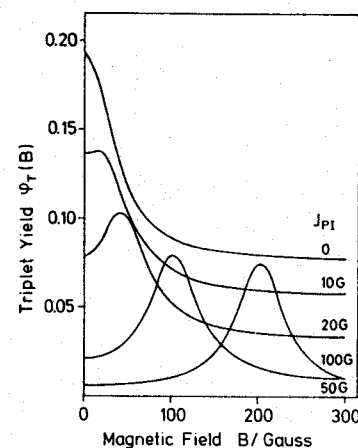


Fig. 12 Magnetic field dependence of the population of  ${}^3\text{Chl}_2^*$  for a  ${}^1({}^2\text{Chl}_2^+ {}^2\text{Ph}^-)$  initial pair for exchange interactions  $J(\text{Chl}_2\text{-Ph}) = 0, 10, 20, 50$  and  $100$  Gauss (from Ref. 8, see details there).

The most relevant information implied in Fig. 11 lies actually in the fact that a magnetic field reduction of the  ${}^3\text{Chl}_2^*$  population is being observed at all. A calculation of the electron spin motion of the  ${}^2\text{Chl}_2^+ {}^2\text{Ph}^-$  pair accounting for a non-vanishing exchange interaction between the two molecular partners yields a very different magnetic field behaviour as illustrated by Fig. 12. In the presence of an exchange interaction the field behaviour reflects mainly a resonance transition between the  $S_0$  and the  $T_-$  state around fields  $B = 2J(\text{Chl}_2\text{-Ph})$  (see Fig. 8). The observations show a field reduction instead of a resonance and pose then an upper

limit on the exchange interaction:  $J(\text{Chl}_2\text{-Ph}) < 10^{-7} \text{ eV} \approx 10 \text{ Gauss}$ . However, the exchange energy is based on the orbital overlap between the molecular partners, the same feature which determines the time scale of the initial photoinduced electron transfer  $^1\text{Chl}_2^* \text{Ph} \rightarrow ^2\text{Chl}_2^+ \text{Ph}^-$  which has been observed to be only about 10 ps. As pointed out by Haberkorn et. al. [10] these two observations cannot be reconciled and, hence, the magnetic field observation forces a revision of the model underlying Fig. 9.

The magnetic field dependence of the  $^3\text{Chl}_2^*$  population can also provide information on the exchange interaction between  $^2\text{Ph}^-$  and  $^2\text{Q}^-$  and thereby information on the  $^2\text{Ph}^- \text{Q}^- \rightarrow ^1\text{Ph}^2\text{Q}^-$  step of the photosynthetic transfer chain. Figure 13 illustrates that the main effect of this exchange interaction is to suppress the magnetic field reduction. This influence of  $J(\text{Ph-Q})$  is due to its action to replace the  $^2\text{Ph}^-$  electron spin of the  $^1[{}^2\text{Chl}_2^+ \text{Ph}^-]$  pair by the randomly oriented  $^2\text{Q}^-$  electron spin and, in this way  $J(\text{Ph-Q})$  contributes to a magnetic field independent channel for the transition  $^1[{}^2\text{Chl}_2^+ \text{Ph}^-] \rightarrow ^3[{}^2\text{Chl}_2^+ \text{Ph}^-]$ .

The spin-dependent electron transfer rates  $k_s$  and  $k_t$  have an effect on the magnetic field behaviour as well. This effect is illustrated in Fig. 14 which demonstrates that the lifetime broadening due to a large  $k_t$  value results in a broader region of near degeneracy of the  $S_0$  and  $T_0$ ,  $T_+$ ,  $T_-$  levels and, hence, leads to an upfield shift of the magnetic field reduction.

The thermally-activated reverse electron transfer  $^1[{}^2\text{Chl}_2^+ \text{Ph}^-] \rightarrow ^1\text{Chl}_2^* \text{Ph}$  with rate constant  $k'_s$  can also contribute to the magnetic field dependence of the reaction center spin dynamics as illustrated by Fig. 15. An increase of the  $k'_s$  value produces an upfield shift of the magnetic field reduction. The presence of this transfer channel implies actually that there should be a magnetic field dependence of the quantum yield of the fluorescence  $^1\text{Chl}_2^* \rightarrow ^1\text{Chl}_2$  or of the fluorescence of other pigments coupled to  $^1\text{Chl}_2^*$  by energy transfer. Such dependence has been observed by Rademaker et. al. [11] as illustrated in Fig. 16.

The magnetic field studies discussed have been extended to other bacterial and plant photosynthetic material and have already contributed much to the understanding of the primary processes of photosynthesis. However, the fact that the electron spin dynamics senses a variety of exchange and electron transfer interactions in the reaction center appears to also pose a limitation on the value of this method: the many contributing factors make it difficult to extract from the observed magnetic field dependence information on a specific interaction [19]. In any case, the basis for an analysis in terms of microscopic interactions in the reaction center is a quantitative theory of the electron spin dynamics. An outline of this theory is presented in the next section.

We have demonstrated above that electron transfer processes which are ubiquitous in the metabolic pathways of biological cells can be influenced by magnetic fields of 10 Gauss. However, there is no reason why fields as weak as the geomagnetic

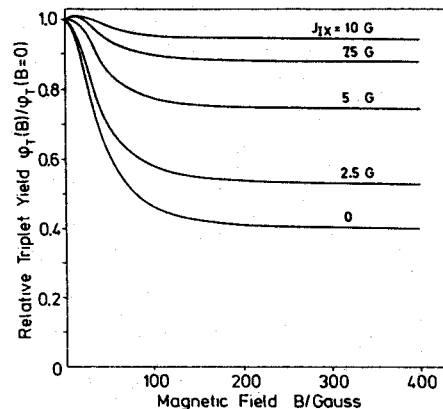


**Fig. 13**  
Magnetic field dependence of the population of  $^3\text{Chl}_2^*$  in an initial  $^1({}^2\text{Chl}_2^+ \text{Ph}^-) \text{ } ^2\text{Q}^-$  system for exchange interactions  $J(\text{Chl}_2\text{-Ph}) = 0$ , and  $J(\text{Ph-Q}) = 0, 2.5, 5, 7.5 \text{ Gauss}$  (from Ref. 8, see details there).

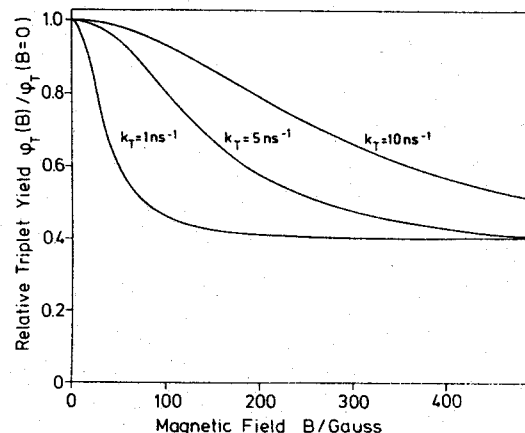


**Fig. 14**  
Magnetic field dependence of the population of  $^3\text{Chl}_2^*$  for a  $^1({}^2\text{Chl}_2^+ \text{Ph}^-)$  initial pair for various decay constants  $k_t$  of the triplet state  $^3({}^2\text{Chl}_2^+ \text{Ph}^-)$ ; the decay constant for the corresponding singlet state is held fixed at  $.1 \text{ ns}^{-1}$  (from Ref. 8, for details see there).

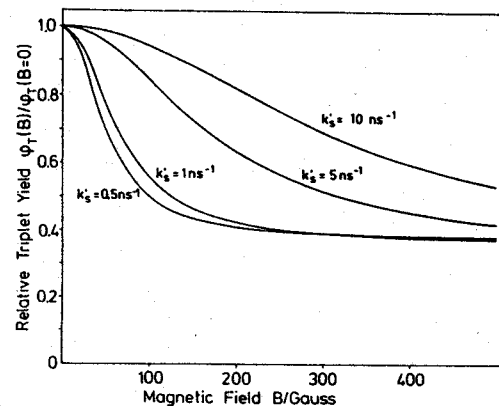


**Fig. 15**  
Magnetic field dependence of the population of  $^3\text{Chl}_2^*$  for a  $^1({}^2\text{Chl}_2^+ \text{Ph}^-)$  initial pair for various rate constants  $k'_s$  of the thermally activated electron transfer  $^1({}^2\text{Chl}_2^+ \text{Ph}^-) \rightarrow ^1\text{Chl}_2^* \text{Ph}$  (from Ref. 8, for details see there).



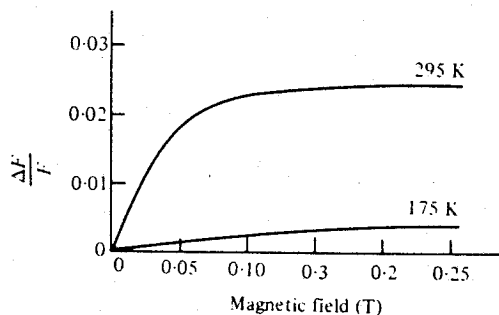


**Fig. 16**  
Magnetic field dependence of the thermaly activated reverse electron transfer  $^1(2\text{Chl}_2^+ 2\text{Ph}^-) \rightarrow ^1\text{Chl}_2^+ 1\text{Ph}^-$  at  $T = 295^\circ\text{K}$  and  $T = 175^\circ\text{K}$  monitored in chromatophores through the fluorescence at  $\lambda > 890\text{ nm}$  (from Ref. 11).

### The Chemical Compass

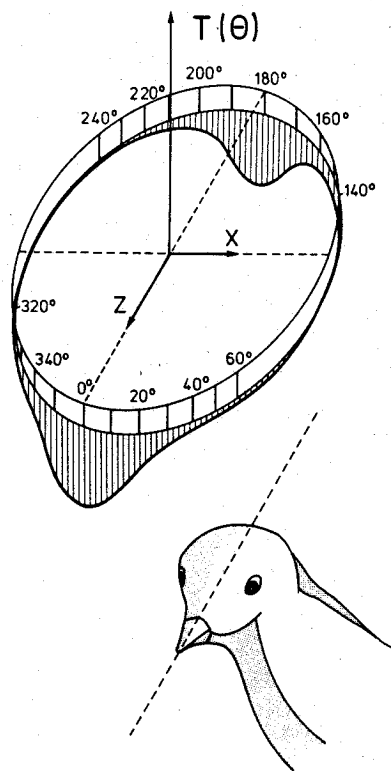
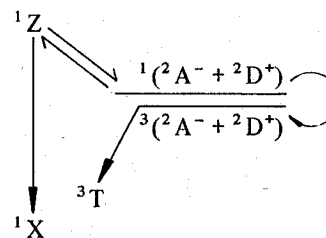


**Fig. 17**  
Mechanism of a biochemical compass: an electron transfer process between doublet pairs  $2\text{A}^- + 2\text{D}^+$  fixed to a spatially oriented biological membrane exhibits a dependence on its orientation in the geomagnetic field in case that a *weak* and *anisotropic* hyperfine coupling is operative; T presents the concentration of a triplet product generated along the pathway  $^1(2\text{A}^- + 2\text{D}^+) \rightarrow ^3(2\text{A}^- + 2\text{D}^+) \rightarrow ^3\text{T}$  (for details see text),  $\theta$  denotes the azimuthal angle in the x, z-plane; the symmetry of the angular dependence of T( $\theta$ ) due to the random orientation of nuclear spins does not allow to determine the polarity of the geomagnetic field; however, interpretation of the inclination of the axial direction of the field lines allows to acquire full orientation (for details see Ref. 12).

field of about .5 Gauss should not also affect such transfer processes. This may lead one to suggest a reaction mechanism for a biochemical compass which exhibits a sensitivity on the orientation of the geomagnetic field. For this purpose one has to assume a *weak* and *anisotropic* hyperfine coupling or very anisotropic and vastly different g-tensors in a doublet pair fixated in a membrane which is well oriented in an organism. As a test of this idea we have studied the following reaction scheme with a singlet  $\rightarrow$  triplet transition induced by anisotropic hyperfine coupling:



anisotropic hyperfine coupling induces an orientational dependence of this transition

In this scheme  $^1\text{Z}$  denotes a singlet precursor for the  $^1(2\text{A}^- + 2\text{D}^+)$  singlet pair; reverse electron transfer populates either  $^1\text{Z}$  or  $^3\text{T}$ , depending on the spin alignment;  $^1\text{Z}$  can decay to  $^1\text{X}$ . In case of an axially-symmetric hyperfine coupling tensor  $\underline{A}$  for a single nuclear spin the system is described by the spin Hamiltonian

$$H = g\mu B \cdot (\underline{S}_1 + \underline{S}_2) + I_z A_{zz} S_{1z} + (I_x S_{1x} + I_y S_{1y}) A_{xx}$$

which enters the appropriate stochastic Liouville equation [12]. For a choice of  $A_{zz} = 4$  Gauss,  $A_{xx} = 5$  Gauss,  $B = 1$  Gauss and some suitable reaction constants one obtains the angular dependence of the population of T shown in Fig. 17. A major question regarding this suggestion of a biochemical compass concerns the nature of the precursor of the pure singlet pair  $^1\text{Z}$  (or for a slightly altered scheme the precursor of a pure triplet pair  $^3\text{Z}$ ). One expects that  $^1\text{Z}$  ( $^3\text{Z}$ ) implies a photoexcited molecule. In this respect it is of interest that the recent search for the magnetic sensor of birds concentrates on the pineal gland (glandula pinealis), a light sensitive organ of the brain.

### 3 Coherent Spin Motion Coupled to Stochastic Degrees of Freedom – Outline of the Theory [13, 14]

The magnetic field modulated electron transfer processes discussed in Sections 1 and 2 entail a coherent electron-nuclear spin motion in concert with stochastic processes: the generation, diffusion and recombination of a doublet pair. The pair is described by a density matrix  $\rho(\underline{r}, t)$  the elements of which provide the population and phases of the electron-nuclear spin states, and the functional dependence

of which accounts for the spatial distribution and time development. The density matrix is the solution of the stochastic Liouville equation

$$\begin{aligned} \frac{\partial}{\partial t} \rho(\underline{r}, t) &= g(\underline{r}, t) \underline{Q}_s && \text{generation} \\ &+ \varrho(\underline{r}) \rho(\underline{r}, t) && \text{diffusion} \\ &- \frac{i}{\hbar} [\underline{H}(\underline{r}), \rho(\underline{r}, t)]_- && \text{spin motion} \\ &- [\underline{U}(\underline{r}), \rho(\underline{r}, t)]_+ && \text{recombination} \end{aligned} \quad (4)$$

In this equation  $g(\underline{r}, t)$  describes the temporal and spatial distribution of the pairs generated through photoinduced electron transfer in the singlet state, the differential operator

$$\varrho(\underline{r}) = \frac{\partial}{\partial \underline{r}} \cdot \underline{D}(\underline{r}) \left[ \frac{\partial}{\partial \underline{r}} - \frac{1}{kT} \underline{F}(\underline{r}) \right] \quad (5)$$

describes the Brownian motion in the force field  $\underline{F}(\underline{r})$ , the matrix  $\underline{H}(\underline{r})$  is the electron-nuclear spin Hamiltonian discussed in Section 1, and the matrix

$$\underline{U}(\underline{r}) = \frac{1}{2} \kappa_s(\underline{r}) \underline{Q}_s + \frac{1}{2} \kappa_t(\underline{r}) \underline{Q}_t \quad (6)$$

represents an optical potential accounting for the depletion of singlet and triplet pairs.  $\underline{Q}_s$  and  $\underline{Q}_t$  are projection operators on the subspace of singlet and triplet electron spin states; furthermore the definition  $[\underline{A}, \underline{B}]_{+/-} = \underline{AB} \pm \underline{BA}$  has been employed. The observables can be readily evaluated once  $\rho(\underline{r}, t)$  is known, e.g. the total fraction of pairs which react to the triplet state by means of the process  ${}^2A^- + {}^2D^+ \rightarrow {}^3A^* + {}^1D$  is

$$c_t = \frac{1}{2} \int_0^\infty dt \int d\underline{r}^3 \kappa(\underline{r}) [\underline{Q}_t, \rho(\underline{r}, t)]_+ \quad (7)$$

Unfortunately, a solution of the stochastic Liouville equation is impossible in general. The difficulty in solving this set of coupled partial differential equations lies in the large number of electron-nuclear spin degrees of freedom, in the spatial degrees of freedom in case the diffusion cannot be assumed to be spherically symmetric, and in the coupling of spatial and spin degrees due to the spatial dependence of  $\underline{H}(\underline{r})$ , and due to the spin dependence of  $\underline{U}(\underline{r})$ . Beside these technical problems there exists also an uncertainty about the spatial dependence of  $g(\underline{r}, t)$ ,  $\kappa_s(\underline{r})$  and  $\kappa_t(\underline{r})$ , i.e. how far do electrons jump (?), as well as about the nature of the force field  $\underline{F}(\underline{r})$  between the  ${}^2A^- + {}^2D^+$  pair in a polar liquid of organic compounds.

Nevertheless, it has been possible to develop reliable approximate solutions to the stochastic Liouville equations. For this purpose one has to adopt approximation schemes different for systems with and without diffusion-like behaviour. In both cases one can take advantage of the observation that in high magnetic fields electron and nuclear spins do not change their magnetic quantum numbers and, hence, for a given distribution of nuclear magnetic quantum numbers  $M_k^{(1)}$  and  $M_q^{(2)}$  on the two partner molecules the electron spin motion is restricted to two electron-nuclear spin states. This encourages experiments to be carried out at high fields. Unfortunately, the magnetic field dependence itself entails a certain amount of information and, since it involves the measurement of a relative change of an observable, this dependence is technically most readily obtained. However, for appreciable differences in the g-values of the doublet partners there is also a significant high field modulation which, in principle, implies the same information as the low field data (see below).

The approximate description of diffusive spin systems is based on the argument that the coupling of spin motion and reaction as well as the coupling of spin motion and spatial motion due to an exchange interaction is restricted to the short moments of encounters between partner molecules. Since the total encounter time is much less than the time spent between encounters at large separations these couplings can be neglected as far as the probability of singlet  $\rightarrow$  triplet transitions is concerned. This leads one to describe a pair by two coupled time-dependent partial differential equations for the total singlet and triplet probabilities  $p_s(\underline{r}, t)$  and  $p_t(\underline{r}, t)$ , respectively, [13, 14]

$$\begin{aligned} \frac{\partial}{\partial t} p_s(\underline{r}, t) &= [\varrho(\underline{r}) - \kappa_s(\underline{r})] p_s(\underline{r}, t) + \dot{p}_s^{(0)} [p_s(\underline{r}, t) + p_t(\underline{r}, t)] \\ \frac{\partial}{\partial t} p_t(\underline{r}, t) &= [\varrho(\underline{r}) - \kappa_t(\underline{r})] p_t(\underline{r}, t) + \dot{p}_t^{(0)} [p_s(\underline{r}, t) + p_t(\underline{r}, t)]. \end{aligned} \quad (8)$$

In order to solve these equations one needs to determine the unperturbed singlet and triplet probabilities  $p_s^{(0)}(t)$  and  $p_t^{(0)}(t) = 1 - p_s^{(0)}(t)$  beforehand. For small nuclear spin systems one can obtain an exact solution. For larger systems the semi-classical approximation underlying Fig. 2 applies and yields a very simple and reliable description. The solution of the time-dependent differential equation may then be conveniently cast in terms of a path integral which can be evaluated by means of a Monte Carlo algorithm [15]. Such an algorithm allows the study of diffusion and reaction processes not restricted to spherical symmetry.

In the case of the photosynthetic reaction center, the doublet partners are in permanent contact and therefore the coupling of spin motion and recombination cannot be neglected. In the high field limit a solution of the corresponding stochastic Liouville equation is possible since the spatial degrees of freedom are omitted (see also below). However, to account for low field situations one has to resort to a rather artificial reduction of the nuclear spin system, i.e. one introduces

a model spin Hamiltonian with very few nuclear spins and (larger) effective hyperfine coupling. Since in the zero field limit the electron spin motion of each doublet is strictly independent, it appears that the most simple model should at least include one nuclear spin on each radical. Such a model has in fact been employed to obtain the results presented in Figs. 12–15. For the sake of an analytical treatment a one nuclear spin model had been suggested too [16].

In order to illustrate this discussion we present for a liquid phase process as well as for a solid state process two models for which the stochastic Liouville equation yields an analytical solution. For a liquid system, i.e. with diffusion, we consider a case in which the recombination process is spin-independent [ $\kappa_s(\underline{r}) = \kappa_t(\underline{r})$ ] and the exchange interaction is negligible. With these restrictions the Liouville equation separates into a diffusion-reaction equation

$$\frac{\partial}{\partial t} p(\underline{r}, t) = \left\{ \frac{\partial}{\partial \underline{r}} D(\underline{r}) \cdot \left[ \frac{\partial}{\partial \underline{r}} - \frac{1}{kT} F(\underline{r}) \right] - \kappa(\underline{r}) \right\} p(\underline{r}, t) \quad (9)$$

and a Schrödinger equation for the spin motion

$$\frac{\partial}{\partial t} \rho(t) = -\frac{i}{\hbar} [H, \rho] \quad (10)$$

For the case of free diffusion [ $F(\underline{r}) = 0$ ], assuming spherical symmetry and generation as well as reaction at the distance of closest approach one obtains for the reaction rate [13]

$$\dot{n}(t) = \int d\underline{r} \dot{p}(\underline{r}, t) = -\frac{\kappa_0}{\sqrt{\pi D t}} \left[ 1 - f\left(\frac{\kappa_0}{\phi_\infty} \sqrt{t/D}\right) \right] \quad (11)$$

where  $f(z) = \sqrt{\pi} z \exp(z^2) \operatorname{erfc}(z)$ ,  $\phi_\infty$  is the total fraction of pairs which recombine and  $\kappa_0$  a reaction constant which describes the electron backtransfer. In the limit of high magnetic field and for a nuclear spin distribution characterized by the set of magnetic quantum numbers  $M_k^{(1)}$  and  $M_k^{(2)}$  the triplet probability is

$$p_t(t) = \frac{1}{2} \sin^2 \omega(\underline{M}, B) t, \quad (12)$$

$$\omega(\underline{M}, B) = \frac{1}{2\hbar} [\mu B (g_1 - g_2) + \sum_k a_k^{(1)} M_k^{(1)} - \sum_k a_k^{(2)} M_k^{(2)}].$$

The fraction of triplet products for the nuclear spin arrangement  $\underline{M} = \{M_k^{(1)}, M_k^{(2)}\}$  is

$$c_t = \int dt \dot{n}(t) p_t(t) = \frac{1}{2} \phi_\infty h[\kappa_0^2 / 2\phi_\infty^2 D \omega(\underline{M}, B)] \quad (13)$$

where

$$h(y) = [1 - \sqrt{y/2} (1 - y)] / (1 + y^2).$$

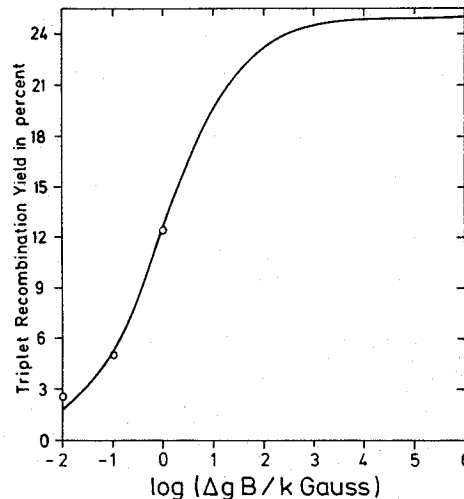


Fig. 18  
Saturation behaviour at very high fields of the fraction of triplet products  $c_t$  of a doublet pair born in a singlet state with  $\Delta g = g_1 - g_2$  (from Ref. 14, for details see text).

For large fields  $c_t$  becomes independent of the hyperfine coupling contribution. The magnetic field dependence of  $c_t$  is illustrated in Fig. 18. The results show a saturation of  $c_t$  which develops when the Zeeman interaction induced singlet  $\rightarrow$  triplet transition is considerably faster than the diffusive separation of the doublet pair. Hence, the observable  $c_t$  at high fields provides similar information as in the low field situation.

In the case of a reaction center system with a doublet pair in permanent contact but with negligible exchange interaction the stochastic Liouville equation in the high field limit

$$\rho(t) = -\frac{i}{\hbar} \left[ \begin{pmatrix} 0 & \omega(\underline{M}, B) \\ \omega(\underline{M}, B) & 0 \end{pmatrix}, \rho \right] - \frac{1}{2} \left[ \begin{pmatrix} \kappa_s & 0 \\ 0 & \kappa_t \end{pmatrix}, \rho \right] + \quad (14)$$

can be solved. The basis is formed by the two states  $S_0, T_0$ . For pairs born in the singlet state one obtains for the fraction of triplet products

$$c_t = -\kappa_t \frac{\omega^2}{\Omega^2} \left[ \frac{1}{(\kappa_s + \kappa_t)^2 - 16 \Omega^2} - \frac{1}{\kappa_s + \kappa_t} \right] \quad (15)$$

where

$$\Omega^2 = \frac{(\kappa_s - \kappa_t)^2}{16} - \omega^2.$$

This expression exhibits a behaviour similar to the one of Fig. 18 and, hence,  $c_t$  in the high field limit also implies information about the electron transfer dynamics of the photosynthetic reaction center. Observations on the high field behaviour of bacterial reaction centers have been obtained by Boxer et. al. [17].

## 4 Conclusion

We have demonstrated above that photoprocesses which involve bimolecular reactions between non-zero spin intermediates, i.e. doublet molecules, can be influenced by external magnetic fields. Such behaviour has also been observed for processes involving triplet pairs and triplet-doublet pairs as in triplet-triplet annihilation  $^3A^* + ^3A^* \rightarrow ^1A^* + ^1A$  and triplet quenching by doublets  $^3A^* + ^2B \rightarrow ^1A + ^2B$ .

The external magnetic field alters a coherent spin motion of the intermediates induced either by the hyperfine interaction in the case of doublets or by the zero field splitting interaction in the case of triplets and thereby produces a change in the population of reaction products. An analysis which combines a description of the spin motion and concomitant stochastic processes can provide new detailed information on the dynamics of the processes involved, e.g. in the photosynthetic reaction center, and has also led to an efficient method of photochemical isotope separation.

Magnetic field studies of molecular processes have experienced a rapid development during the past years and in this lecture we have only provided examples closely connected with our own work. For completeness we mention the application of alternating magnetic fields on bimolecular processes and the observation of field effects on intramolecular gas phase processes. Closely related is also the benchmark work of Stehlik and coworkers [18] on the effect of optical nuclear polarization. Now that magnetic field studies have gained reputation the future appears to hold great promise for this expanding area of activities.

## Acknowledgement

The author likes to thank A. Weller and his former colleagues at the Max-Planck-Institute for Biophysical Chemistry for the pleasure and the privilege to collaborate on the subject of this lecture.

## References

- [1] A.R. Lepley and G.L. Closs, Eds. 'Chemically Induced Magnetic Polarization', John Wiley (New York, 1973).
- [2] K. Schulten, H. Staerk, A. Weller, H.-J. Werner, and B. Nickel, Z. Phys. Chem. NF 101, 37 (1976).
- [3] K. Schulten and P.G. Wolynes, J. Chem. Phys. 68, 3292 (1978); E.-W. Knapp and K. Schulten, J. Chem. Phys. 71, 1878 (1979).
- [4] H.-J. Werner, H. Staerk, and A. Weller, J. Chem. Phys. 68, 2419 (1978).
- [5] H.W. Krüger, M.E. Michel-Beyerle, and H. Seidlitz, Chem. Phys. Lett. 87, 72 (1982); F. Nolting, H. Staerk, and A. Weller, Chem. Phys. Lett. (in press).
- [6] Actually, there is also a weak magnetic field dependence expected for random encounters, for details see Ref. 2.
- [7] N.J. Turro and B. Kraeutler, J. Am. Chem. Soc. 100, 7432 (1978); N.J. Turro, B. Kraeutler, and D.R. Anderson, J. Am. Chem. Soc. 101, 7435 (1979); B. Kraeutler and N.J. Turro, Chem. Phys. Lett. 70, 266, 270 (1980).
- [8] H.-J. Werner, K. Schulten, and A. Weller, Biochim. Biophys. Acta 502, 255 (1978).
- [9] A.J. Hoff, R. Van Grondelle and L.N.M. Duysens, Biochim. Biophys. Acta 460, 547 (1977); for a most recent review see A.J. Hoff, Quart. Rev. Biophys. 14, 599 (1981).
- [10] R. Haberkorn, M.E. Michel-Beyerle and R. Marcus, Proc. Natl. Acad. Sci. USA 76, 4185 (1979).
- [11] H. Rademaker, A.J. Hoff, and L.N.M. Duysens, Biochim. Biophys. Acta 546, 248 (1979).
- [12] K. Schulten, Ch.E. Swenberg, and A. Weller, Z. Phys. Chem. NF 111, 1 (1978); as an example for the observation of magnetic orientation in migratory birds see W. Wiltshcko and R. Wiltshcko, Science 176, 62 (1972); the magnetic navigation in bacteria which appears to rely on a different mechanism has been reviewed in R.P. Blakemore and R.B. Frankel, Sci. Am. 245, 42 (1981).
- [13] Z. Schulten and K. Schulten, J. Chem. Phys. 66, 4676 (1977).
- [14] H.-J. Werner, Z. Schulten, and K. Schulten, J. Chem. Phys. 67, 646 (1977).
- [15] K. Schulten and I. Epstein, J. Chem. Phys. 71, 309 (1979); further developments of the Monte Carlo algorithms for diffusion processes can be found in G. Lamm and K. Schulten, J. Chem. Phys. 75, 365 (1981); *ibid.* (submitted for publication).
- [16] R. Haberkorn and M.E. Michel-Beyerle, Biophys. J. 26, 489 (1979).
- [17] C.E.D. Chidsey, M.G. Roelofs, and S.G. Boxer, Chem. Phys. Lett. 74, 113 (1980).
- [18] J.P. Colpa, F. Steif, and D. Stehlik, Chem. Phys. 33, 79 (1978) and references therein.
- [19] Recently, M.G. Roelofs, C.E.D. Chidsey, and S.G. Boxer, Chem. Phys. Lett. 87, 582 (1982) suggested also an important role of the fine structure interaction, i.e. the dipolar electron spin-spin interaction through space between  $^2\text{Chl}_2^+$  and  $^2\text{Ph}^-$ ; this interaction has been accounted for by the authors in the framework of the theory outlined here and in [8].